Probing Side Chain Dynamics of Branched Macromolecules by Pyrene Excimer Fluorescence

Shiva Farhangi, Jean Duhamel*

Institute for Polymer Research, Waterloo Institute for Nanotechnology, Department of Chemistry, University of Waterloo, 200 University Avenue West, Waterloo, ON N2L 3G1, Canada

* To Whom correspondence should be addressed

ABSTRACT

Four different pyrene-labeled polymers were prepared by radical copolymerization of n-butyl methacrylate (BMA) and 1-pyrenemethyl methacrylate ($PyEG_0MA$), 1-pyrenemethoxyethyl methacrylate ($PyEG_1MA$), 1-pyrenemethoxyethoxyethyl methacrylate ($PyEG_2MA$), and 1-pyrenemethoxydiethoxyethyl methacrylate ($PyEG_3MA$) to yield $PyEG_0$-PBMA, $PyEG_1$-PBMA, $PyEG_2$-PBMA, and $PyEG_3$-PBMA, respectively. The only structural difference between the polymers was the length of the oligo(ethylene glycol) spacer separating the pyrene label from the main chain. Steady-state and time-resolved fluorescence were applied to investigate how the length of the spacer affected the photophysical properties of the pyrene-labeled polymers. Excimer formation between an excited and a ground-state pyrene was enhanced by a longer spacer which increased the probability of encounter between two pyrene labels. This conclusion was supported through the analysis of the fluorescence decays of the polymers according to the Fluorescence Blob Model (FBM) which yielded the number (N_{blob}) of monomers constituting the volume in the polymer coil probed by an excited pyrene and the rate constant of excimer formation, k_{blob}, inside a *blob*. N_{blob} increased more or less linearly with increasing spacer length reflecting a larger *blob* volume. k_{blob} for $PyEG_0$-PBMA was small due to steric hindrance while k_{blob} took a larger but similar value within experimental error for all polymers labeled with pyrene derivatives having oligo(ethylene glycol) spacers. These experiments demonstrate that for a branched macromolecule, the volume probed by the tip of a side chain and its dynamics can be characterized quantitatively by monitoring pyrene excimer fluorescence. They are expected to provide important dynamic and structural information about the numerous highly branched macromolecules that are currently under intense scientific scrutiny.

INTRODUCTION

Polymeric bottlebrushes,[1-3] dendrimers,[4,5] or comb[6] and arborescent[7] polymers are all examples of highly branched macromolecules (HBMs) that can be prepared in a well-defined manner and whose architecture endows them with a broad range of highly sought after properties for catalysis,[4] drug delivery,[5] or enhanced lubrication at interfaces,[8] as contrast agents for imaging[9] or associative thickeners in paints.[10] If one focuses on anisotropic HBMs such as comb polymers or polymeric bottlebrushes, their characterization presents experimentalists with an additional challenge compared to linear chains since in theory, this characterization should be conducted along two perpendicular directions, one running axially along the main chain and the other running perpendicularly to the main axis along the side chain. In practice, the characterization of HBMs relies usually on the determination of their overall mass by a combination of techniques such as NMR, gel permeation chromatography, or static light scattering followed by the characterization of their dimensions in solution by scattering or intrinsic viscosity measurements.[11-13] While such studies provide an accurate description of the averaged properties of HBMs in terms of their hydrodynamic or gyration radii for example, they do not yield much detailed information about the actual behavior of the side chains. Microscopy which provides the dimensions of polymeric bottlebrushes adsorbed onto a substrate along their main and secondary axes might be currently the only technique to characterize HBMs adsorbed onto a two-dimensional substrate along two different axes[13] but it does not provide much information about the behavior of the side chains of HBMs adopting their natural three-dimensional conformation in solution.

Over the years, experiments on linear chains labeled randomly or at their ends with the dye pyrene have established that polymer chain dynamics and the volume probed by an excited pyrene could be measured quantitatively by characterizing the kinetics of excimer formation between an

excited and a ground-state pyrene according to the Fluorescence Blob Model (FBM) for randomly labeled polymers[14-17] or Birks' scheme for end-labeled chains.[18,19] The present report investigates whether pyrene excimer fluorescence which enables the thorough characterization in solution of the internal dynamics of linear chains labeled with pyrene could also probe the dynamics of side chains in the direction perpendicular to the main chain. To this end, four series of poly(butyl methacrylate) (PBMA) were prepared by copolymerizing BMA with four pyrene-labeled monomers where a 1-pyrenemethoxide label was connected to a methacrylate monomer via 0 – 3 ethylene glycol units. In so doing, the pyrene label was held at increasing distances from the main chain and its efficiency at forming excimer was characterized as a function of side chain length. Surprisingly, increasing the side chain length was found to dramatically enhance the ability of the pyrene-labeled PBMA constructs to form excimer. The cause for the large enhancement in pyrene excimer formation was clearly identified by analyzing the fluorescence decays of the four series of pyrene-labeled PBMA with the FBM. With increasing side chain length, the pyrene labels were held further away from the slow moving main chain allowing them to experience an enhanced mobility and an increased probability of undergoing pyrene–pyrene encounters due to the longer reach of the spacer. Based on these results, the experiments described herein suggest that pyrene excimer fluorescence represents an effective means to probe in solution the dynamics of the side chains of the many HBMs that are under current investigation.

EXPERIMENTAL

Materials: 1-(Bromomethyl)pyrene, 1-pyrenemethanol, silver(I) oxide (Ag_2O), diethylene glycol (DEG), and triethylene glycol (TEG) were purchased from Sigma-Aldrich. Celite 545 Filter Aid Powder was provided by Fisher Scientific. Distilled in glass tetrahydrofuran (THF) was supplied

by Caledon Laboratories. Four PBMA standards with narrow molecular weight polydispersity (M_n in kg.mol^{-1} (PDI) = 7.0 (1.6), 13 (1.12), 24 (1.25), and 38 (1.15)) were purchased from Polymer Source and one PBMA standard (M_n = 2.8 kg.mol^{-1} (PDI=1.15)) from PSS. All chemicals were used as received.

Synthesis of 1-pyrenemethyloxyethyl methacrylate (PyEG$_1$-MA): The synthesis of this pyrene-labeled monomer has been described elsewhere.[20]

Synthesis of 1-pyrenemethoxyethoxy ethanol (PyEG$_2$-OH) and 1-pyrenemethoxydiethoxy ethanol (PyEG$_3$-OH): The same procedure was applied for both compounds. Only the synthesis of PyEG$_2$-OH is described in details hereafter. DEG (1.00 g, 5.82 mmol) was added to a suspension of Ag_2O (1.97 g, 8.5 mmol) in 25 mL of dichloromethane (DCM) under a flow of nitrogen and the solution was stirred for 45 minutes under nitrogen. 1-(Bromomethyl)pyrene (1.83 g, 6.20 mmol) was dissolved in 5 mL DCM and the solution was added drop wise to the reaction mixture. The reaction was stirred under nitrogen at room temperature for 72 hours. After the reaction, the solution was filtered through a Celite® bed. The solvent was removed with a rotary evaporator and the yellow remaining residue was purified by silica gel column chromatography using a 55:45 ethyl acetate-to-hexane mixture. A pale-yellow oil was obtained in a 45% yield. The ^{1}H NMR spectra of PyEG$_2$-OH and PyEG$_3$-OH are shown in Figures S1 and S2, respectively.

300 MHz ^{1}H NMR (DMSO-d$_6$) for PyEG$_2$-OH: δ 3.41-3.71 (m, 8H, O-CH$_2$-CH$_2$-O-CH$_2$-CH$_2$-O), δ 4.6 (t, 1H, OH), δ 5.2 (s, 2H, py-CH$_2$-O), δ 8.0-8.4 (m, 9H, Py H's).

300 MHz ^{1}H NMR (DMSO-d$_6$) for PyEG$_3$-OH: δ 3.37-3.72 (m, 12H, O-CH$_2$-CH$_2$-O-CH$_2$-CH$_2$-O-CH$_2$-CH$_2$-OH),δ 4.56 (t, 1H, OH), δ 5.2 (s, 2H, -CH$_2$-O), δ 7.9-8.4 (m, 9H, Py H's).

Synthesis of 1-pyrenemethyl methacrylate (PyEG$_0$-MA), 1-pyrenemethoxyethoxyethyl methacrylate (PyEG$_2$-MA), and 1-pyrenemethoxyethoxydiethyl methacrylate (PyEG$_3$-MA): Only

the synthesis of $PyEG_2MA$ is described in detail since a similar procedure was applied for the synthesis of $PyEG_0$-MA and $PyEG_3$-MA. $PyEG_2$-OH (1.10 g, 3.43 mmol) was dissolved in 30 mL of DCM in a 100 mL round bottom flask. Freshly distilled trimethylamine (1.04 g, 12 mmol) was added to the reaction mixture. The solution was purged with nitrogen for 20 minutes and kept on dry ice. Methacryloyl chloride (0.62 g, 6.0 mmol) was added drop wise. The reaction mixture was brought to room temperature and the solution was stirred under nitrogen for 24 hrs. After the reaction was complete, the reaction mixture was washed with an aqueous solution of 0.5 M HCl, saturated sodium carbonate, and saturated sodium chloride, followed by water in that sequence. A rotary evaporator was used to remove the solvent. The remaining crude product was purified by silica gel column chromatography using a 60:40 ethyl acetate-to-hexane mixture to obtain a yellow oil in 90% yield. The overall synthetic procedure is shown in Scheme 1. The ^{1}H NMR spectra of $PyEG_0$-MA, $PyEG_2$-MA, and $PyEG_3$-MA are shown in Figures S3, S4, and S5, respectively.

300 MHz ^{1}H NMR ($CDCl_3$) for $PyEG_0$-MA: δ 1.95 (s, 3H, CH_3-), δ 5.5 (s, 1H, $=CH_2$), δ 5.9 (s, 2H, Py-CH_2-), δ 6.4 (s, 1H, $=CH_2$), δ 7.9-8.3 (m, 9H, Py H's).

300 MHz ^{1}H NMR ($CDCl_3$) for $PyEG_2$-MA: δ 1.81 (s, 3H, CH_3-), δ 3.73-3.77 (m, 6H, -CH_2-O-CH_2-CH_2-O-), δ 4.29-4.32 (m, 2H, COO-CH_2-), δ 5.2 (s, 2H, Py-CH_2-), δ 5.5 (s, 1H, $=CH_2$), δ 6.1 (s, 1H, $=CH_2$), δ 7.9-8.4 (m, 9H, Py H's).

300 MHz ^{1}H NMR ($CDCl_3$) for $PyEG_3$-MA: δ 1.89 (s, 3H, CH_3-), δ 3.8-4.4 (m, 8H, CH_2-O-CH_2-CH_2-O-CH2-CH2-O), δ 4.21-4.28 (m, 2H, COO-CH_2-), δ 5.2 (s, 2H, Py-CH_2-), δ 5.5 (s, 1H, $=CH_2$), δ 6.1 (s, 1H, $=CH_2$), δ 7.9-8.4 (m, 9H, Py H's).

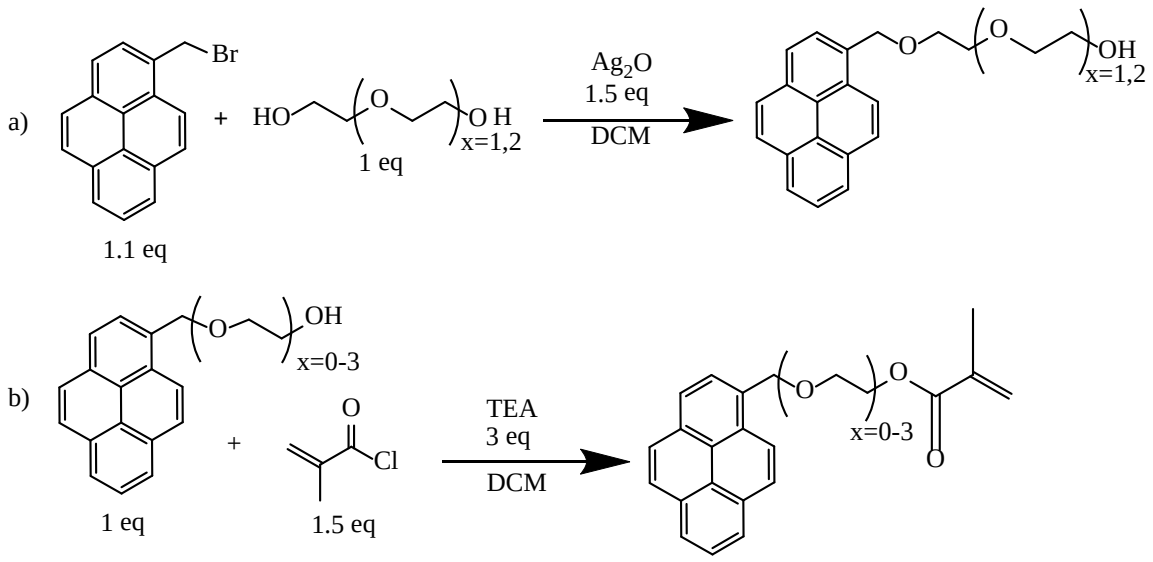

Scheme 1. Synthetic procedure applied to prepare a) $PyEG_2$-OH and $PyEG_3$-OH and b) the monomer series $PyEG_x$-MA with $x = 0 – 3$.

Random copolymerization: The pyrene-labeled poly(butyl methacrylate)s (Py-PBMA) were prepared by radical copolymerization of $PyEG_0MA$, $PyEG_1MA$, $PyEG_2MA$, or $PyEG_3MA$ with butyl methacrylate (BMA) to yield $PyEG_x$-PBMA with $x = 0 – 3$ (structures shown in Table 1) according to a procedure that was developed earlier.[20,21] The synthesis and purification of the $PyEG_x$-PBMA samples with $x = 1$ has been described in detail earlier and the same procedure was applied to prepare the $PyEG_x$-PBMA samples with $x = 0$, 2, and 3.[21]

Table 1. Chemical structure, pyrene content, absolute M_n, and PDI values of the $PyEG_x$-PBMA samples with $x = 0 – 3$.

$PyEG_0$PBMA				**$PyEG_1$PBMA**			
Chemical Structure	Py-content μmol/g (mol %)	M_n kg/mol	PDI	Chemical Structure	Py-content μmol/g (mol %)	M_n kg/mol	PDI
	25 (0.35)	182	1.92		23 (0.32)	164	2.00
	270 (4.0)	204	1.44		123 (1.8)	160	1.80
	352 (5.3)	170	1.39		184 (2.7)	117	2.00
	412 (6.3)	183	1.92		255 (3.8)	100	2.23
	461 (7.1)	164	1.94		304 (4.6)	190	1.73
	525 (8.1)	138	2.20		354 (5.4)	303	1.46
$PyEG_2$PBMA				**$PyEG_3$PBMA**			
Chemical Structure	Py-content μmol/g (mol %)	M_n kg/mol	PDI	Chemical Structure	Py-content μmol/g (mol %)	M_n kg/mol	PDI
	22 (0.32)	179	1.96		23 (0.32)	113	1.56
	123 (1.8)	178	1.56		70 (1.0)	201	1.53
	160 (2.3)	173	1.77		126 (1.9)	117	1.60
	215 (3.2)	191	1.74		142 (2.1)	137	1.48
	258 (3.9)	167	1.56		185 (2.8)	195	1.55
	342 (5.3)	178	1.76		274 (4.2)	157	1.82

Molecular weight determination: Gel Permeation Chromatography (GPC) was applied to determine the absolute molecular weight of the pyrene labeled polymers. A Viscotek GPC 305 Triple Detector Array device with a combination of refractive index (DRI), viscosity, and UV-Vis

absorption detectors was used. The quality and purity of the fluorescently labeled samples, particularly the confirmation that no free pyrene-labeled monomer eluting with the solvent remained in the polymer sample, was achieved by visual inspection of the traces of the DRI and UV-Vis absorption detectors. Examples of GPC traces of the labeled polymers have been presented in Figure S6 in SI. Pyrene content, absolute number average molecular weight (M_n), and polydispersity indices (PDIs) have been listed in Table 1.

Absorption measurements: The absorption spectra used to determine the pyrene content of the $PyEG_x$-PBMA samples and the pyrene concentration ([*Py*] = 2.5×10^{-6} M) for the $PyEG_x$-PBMA solutions used for fluorescence measurements were acquired with a Varian Cary 100 Bio spectrophotometer. The pyrene contents listed in Table 1 were obtained in terms molar fraction (x) of pyrene-labeled monomer and number of moles of pyrene labeled monomer per gram of polymer (λ_{Py} in μmol.g^{-1}). Taking the ratio of the massic polymer concentration in g.L^{-1} over the pyrene concentration in mol.L^{-1} obtained by applying Beer-Lambert law to the solution absorbance with the molar absorption coefficient of 1-pyrenemethanol in THF (ε[344 nm] = 42,700 M^{-1}.cm^{-1}) yielded the parameter λ_{Py}. The molar fraction x of pyrene-labeled monomers could be determined by applying Equation 1 where M_{BMA} is the molar mass of *n*-butyl methacrylate (142 g.mol^{-1}), and M_{Py} is the molar mass of the pyrene-labeled monomers equal to 300, 344, 388, and 432 g.mol^{-1} for $PyEG_0$-MA, $PyEG_1$-MA, $PyEG_2$-MA, and $PyEG_3$-MA, respectively.

$$x = \frac{M_{BMA}}{1/\lambda_{Py} + M_{BMA} - M_{Py}} \quad (1)$$

Steady-state fluorescence: The fluorescence spectra of the dilute $PyEG_x$-PBMA solutions in THF ([*Py*] = 2.5×10^{-6} M) were acquired with a Photon Technology International LS-100 steady-state fluorometer using the right angle geometry. The solutions were excited at 344 nm with an Ushio UXL-75 Xenon lamp and the fluorescence monitored with a PTI 814 photomultiplier. The polymer solutions were outgased with a gentle flow of nitrogen for 30 min. to avoid oxygen quenching. Fluorescence quantum yield measurements were carried out by comparing the fluorescence signal of a polymer sample in THF integrated over the entire fluorescence spectrum with that of 1-pyrenebutanol in THF taking advantage of its known quantum yield (ϕ_{PyBut} = 0.52).[22] The absorption at 344 nm where the 1-pyrenemethoxy derivative absorbs for the solutions used for quantum yield measurements was kept at 0.05.

Time-resolved fluorescence: The same polymer solutions used for steady-state fluorescence measurements were then placed in an IBH Ltd. time-resolved fluorometer to acquire the pyrene monomer and excimer decays at 375 and 510 nm, respectively. The solutions were excited at 344 nm with an IBH 340 nm NanoLED. A 370 and 495 nm cut-off filters were employed to minimize straight light scattering when collecting the monomer and excimer decays, respectively. The fluorescence decays were fitted globally according to the Fluorescence Blob Model (FBM).[15-17,20,21] The quality of the fits was assessed from the χ^2 value (< 1.3) and the random distribution around zero of the residuals and autocorrelation of the residuals. The fits yielded the molar fractions of the different pyrene species present in the solution and the FBM parameters. A more detailed description of the FBM analysis can be found in Supporting Information (SI) and in earlier publications. [15-17,20,21]

RESULTS

Three pyrene derivatives ($PyEG_x$-OH with $x = 1 – 3$) were synthesized by extending the substituent of 1-pyrenemethanol ($PyEG_0$-OH) with one, two, and three ethylene glycol units. Reaction of the $PyEG_x$-OH ($x = 0 – 3$) compounds with methacryloyl chloride yielded four pyrene-labeled methacrylate monomers, which after copolymerization with butyl methacrylate yielded four different polymers ($PyEG_x$-PBMA with $x = 0 – 3$). The fluorescent pyrene label was held at different distances from the main chain by oligo(ethylene glycol) spacers of increasing length to probe whether the formation of excimer between two pyrene labels attached at the tip of the side chains would be affected by the spacer length. All fluorescence spectra of the $PyEG_x$-PBMA samples in THF can be seen in Figure S7. The steady-state fluorescence spectra of a dilute THF solution of the $PyEG_x$-PBMA with $x = 0 – 3$ having a similar pyrene content of about 4 mol% are shown in Figure 1. To avoid intermolecular excimer formation, all fluorescence experiments were conducted with dilute solutions of the $PyEG_x$-PBMA samples in THF using a pyrene concentration of 2.5×10^{-6} M. Figure 1 demonstrates that increasing the spacer length of the pyrene derivative from three atoms in $PyEG_0$-MA to 12 atoms in $PyEG_3$-MA substantially increased the efficiency of pyrene excimer formation. However this conclusion needs to be adjusted to account for the differences in vibrational structure experienced by the pyrene labels in different polymeric constructs. As can be seen in Figure 1, the I_1/I_3 ratio of the pyrene labels equals 1.86 for $PyEG_0$-PBMA but only 1.25, 1.36, and 1.19 for $PyEG_1$-PBMA, $PyEG_2$-PBMA, and $PyEG_3$-PBMA, respectively The fluorescence quantum yield was determined for all solutions in Figure 1 and found to take a similar value of 0.31 ± 0.05. The unnormalized fluorescence spectra used for Figure 1 are presented in Figure S7 in SI.

.

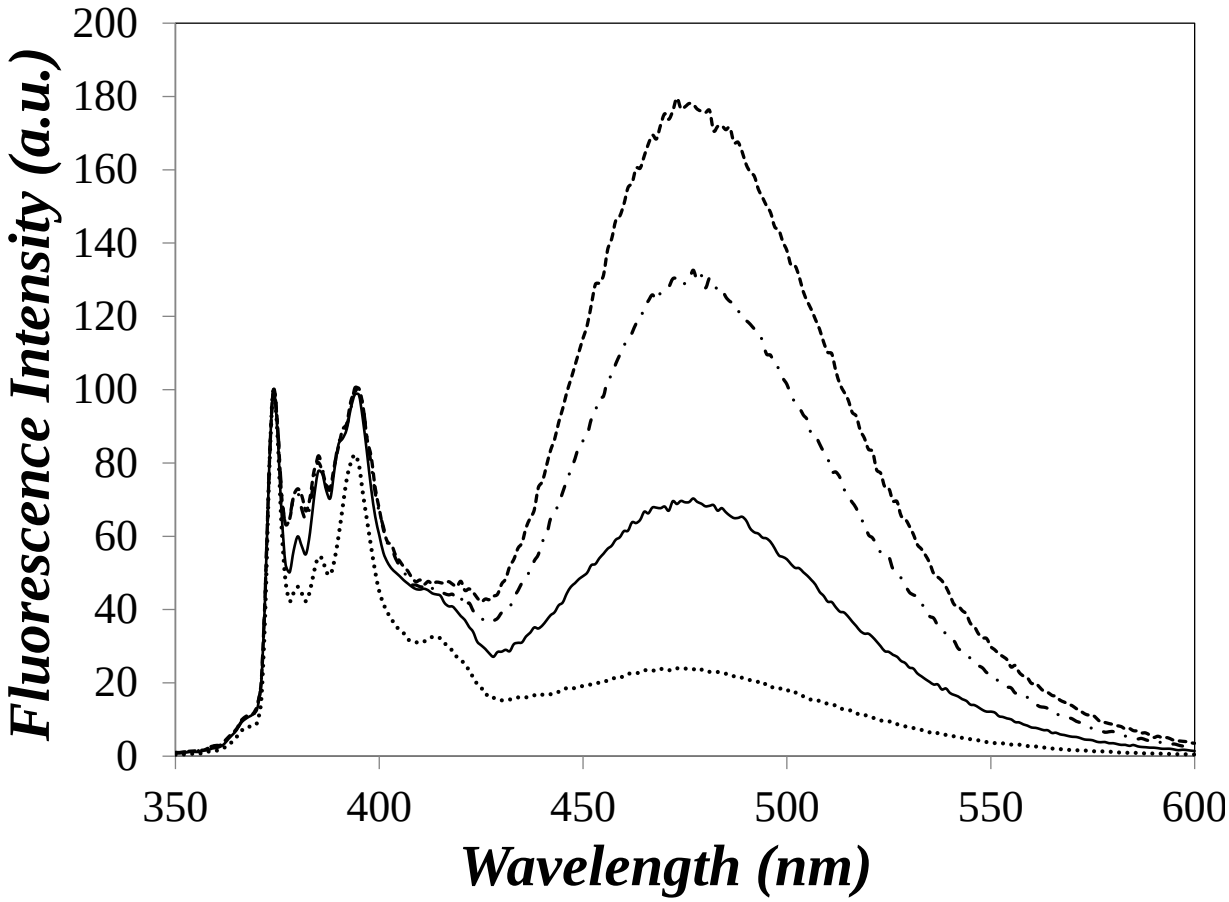

Figure 1. Normalized steady-state fluorescence spectra of (…., ϕ_F = 0.38) Py(4.0)EG_0-PBMA, (—, ϕ_F = 0.27) Py(3.8)EG_1-PBMA, (-.-, ϕ_F = 0.32) Py(3.9)EG_2-PBMA, and (----, ϕ_F = 0.28) Py(4.2)EG_3-PBMA in THF. [*Py*] = 2.5×10^{-6} M, λ_{ex} = 344 nm.

As demonstrated in an earlier publication,[20] the 1-pyrenemethoxy group of $PyEG_1$-OH responds effectively to the polarity of its local environment and so do $PyEG_2$-OH and $PyEG_3$-OH. The similar I_1/I_3 ratios taken by $PyEG_x$-PBMA with x = 1 – 3 suggests that these three constructs respond in a similar manner to the polarity of THF. Since the I_1/I_3 ratio takes a value substantially larger for $PyEG_0$-PBMA, it suggests that either the pyrene label of $PyEG_0$-PBMA probes an environment that is much more polar than THF or that this pyrene derivative responds differently

to the polarity of its environment resulting in a larger I_1/I_3 ratio. As it turns out, the latter possibility is certainly more likely. 1-Pyrenemethanol and 1-pyrenemethyl methacrylate showed an I_1/I_3 ratio of, respectively, 1.76 and 1.83 in THF, similar to the value of 1.86 obtained for $PyEG_0$-PBMA in THF. It is certainly the difference in chemical structure between 1-pyrenemethanol ($PyEG_0$-OH) and the family of $PyEG_x$-OH ($x = 1 – 3$) constructs that leads to the difference in I_1/I_3 ratio between 1.86 for the former and 1.27 ± 0.09 for the latter, a result of the sensitivity of the 0-0 transition of pyrene to the polarity of the environment. In turn, this effect makes it difficult to assess the efficiency of excimer formation for the $PyEG_0$-PBMA series since the larger I_1 peak of $PyEG_0$-PBMA makes the excimer signal of this polymer series appear smaller in Figure 1. Nevertheless, the I_E/I_M ratios of all fluorescence spectra were determined by taking the ratio of the integrals between 500 and 530 nm and between 372 and 378 nm for I_E and I_M, respectively. The I_E/I_M ratios were plotted in Figure 2A as a function of pyrene content.

For each polymer series, the I_E/I_M ratio increased with increasing pyrene content as expected since a larger pyrene content enabled more pyrene encounters and thus more excimer formation. The trend observed in Figure 1 for a pyrene content close to 4 mol% that showed an increase in excimer formation with increasing number of EG units (x) could be generalized as the I_E/I_M ratio in Figure 2A was shown to increase with increasing x value at any pyrene content. Approximating the trends obtained in Figure 2A for the plots of I_E/I_M versus pyrene content as straight lines, the slopes $m(I_E/I_M)$ of these lines were plotted in Figure 2B as a function of the number of atoms in the side chain. The slope $m(I_E/I_M)$ increased linearly with increasing number of atoms in the side chain, thus demonstrating enhanced efficiency of excimer formation displayed by the polymer series prepared with larger oligo(ethylene glycol) linkers. It appears that a larger spacer enabled an excited pyrene to sample a larger volume in the polymer coil thus leading to a

greater probability of encountering a ground-state pyrene and forming an excimer. However since the I_1/I_3 ratio of the $PyEG_0$-PBMA series is much larger than that of the other polymers, these conclusions were true for the three $PyEG_x$-PBMA series with $x = 1 – 3$ that all exhibited a similar I_1/I_3 ratio but might not fully hold for the $PyEG_0$-PBMA series whose I_1 peak was enhanced. By comparison, the time-resolved fluorescence experiments are more straightforward to interpret as their analysis is impervious to the polarity of the environment as it solely reflects the kinetics of pyrene excimer formation. Furthermore, the analysis of the fluorescence spectra of the pyrene-labelled polymers in solution only provides a qualitative measure of their ability to form an excimer since they do not distinguish between the different pyrene species present in solution, namely those pyrenes that are attached onto macromolecular units that diffuse slowly (Py_{diff}), rearrange quickly with a large rate constant k_2 to form an excimer after two slowly diffusing pyrene-bearing macromolecular units have been brought into close proximity (Py_{k2}), cannot form excimer because they are located in pyrene-poor regions of the polymer coil and behave as if they were free in solution (Py_{free}), or are pre-associated and form an excimer (E^*) or an excited long-lived dimer (D^*) instantaneously upon direct excitation of a pyrene dimer. Since the global FBM analysis of the monomer and excimer fluorescence decays can distinguish between those different pyrene species, it can isolate the contribution of Py_{diff} to provide a quantitative measure of the rate constant of diffusive encounters (k_{blob}) between two macromolecular units bearing a pyrene label and the number of backbone monomers encompassing a *blob* (N_{blob}).[15-17,20,21]

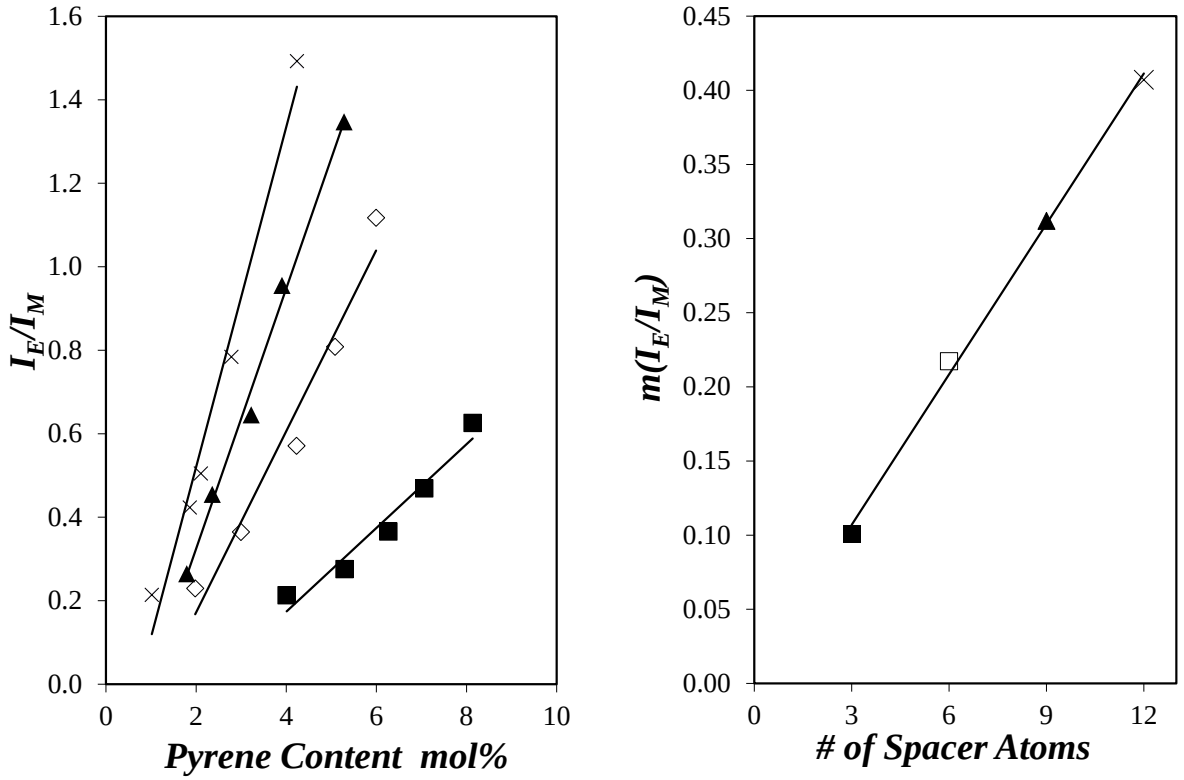

Figure 2. A) Comparison of the I_E/I_M ratios of (■) $PyEG_0$-PBMA labeled with 4.0, 5.3, 6.3, 7.1, and 8.1 mol% pyrene, (◇) $PyEG_1$-PBMA labeled with 1.8, 2.7, 3.8, 4.6, and 5.4 mol% pyrene, (■) $PyEG_2$-PBMA with 1.8, 2.3, 3.2, 3.9, and 5.3 mol% pyrene, and (×) $PyEG_3$-PBMA labeled with 1.0, 1.8, 2.1, 2.7, and 4.3 mol% pyrene. B) $m(I_E/I_M)$ for the same polymers in THF. [*Py*] = 2.5×10^{-6} M, λ_{ex} = 344 nm.

Consequently the fluorescence decays of the pyrene monomer and excimer of all pyrene labeled polymer series were acquired and fitted globally with Equations S1 and S2 according to the FBM analysis. This analysis yielded k_{blob} and N_{blob}, the number of monomers constituting the polymer segment encompassed inside $V_{blob,}$ the volume of a blob, and these parameters will be discussed in detail hereafter. The fits of the decays were excellent as can be seen in Figure S9 in SI. All parameters retrieved from the FBM analysis of the fluorescence decays have been listed

in Tables S3-5 in SI. A more complete description of the FBM can be found in earlier publications.[20,21] The largest molar fractions were f_{diff} and f_{k2} whose combined value ($f_{diff} + f_{k2}$) for all PyEG$_x$-PBMA polymers averaged 0.87 ± 0.03 indicating that the vast majority of pyrene labels formed excimer by diffusion. Thus these fluorescence experiments reflected the diffusive motion of the pyrene terminated side chains.

The FBM analysis of the fluorescence decays also yielded the average number of pyrenes per *blob*, $<n>$. Using the known pyrene content (λ_{Py}) of the polymers listed in Table 1, the number of monomer units encompassed inside a *blob*, N_{blob}, could be determined according to Equation 2.

$$N_{blob} = \frac{1}{(1 - f_{Mfree})} \times \frac{< n >}{x} \qquad (2)$$

In Equation 2, x is the molar fraction of pyrene-labeled monomer of the PyEG$_x$-PBMA samples listed in Table 1. The FBM parameters N_{blob}, k_{blob}, and the product $k_{blob} \times N_{blob}$ obtained from the FBM analysis of the fluorescence decays acquired with each PyEG$_x$-PBMA polymer are shown as a function of pyrene content for the four polymer series in Figures 4A-C. Within experimental error, these parameters remained constant with pyrene content. As usually done in such a situation,[15-17,20,21] their values were then averaged for each polymer series and $<N_{blob}>$, $<k_{blob}>$, and $<k_{blob} \times N_{blob}>$ were plotted in Figures 4D-F as a function of the linker length connecting pyrene to the PBMA chain.

In Figure 3D, $<N_{blob}>$ was found to increase linearly with increasing linker length from 40.5 ± 2.3 for PyEG$_0$-PBMA to 82.7 ± 3.7 for PyEG$_3$-PBMA. This trend indicated that the volume probed by an excited pyrene V_{blob} increased with increasing spacer length as would be expected since a longer spacer allows an excited pyrene to probe a larger volume inside the polymer coil.

The smallest N_{blob} value was obtained for the short 3 atom spacer of the $PyEG_0$-PBMA series which restricted the mobility of the excited pyrene label so that it probed the smallest volume V_{blob} of all other constructs.

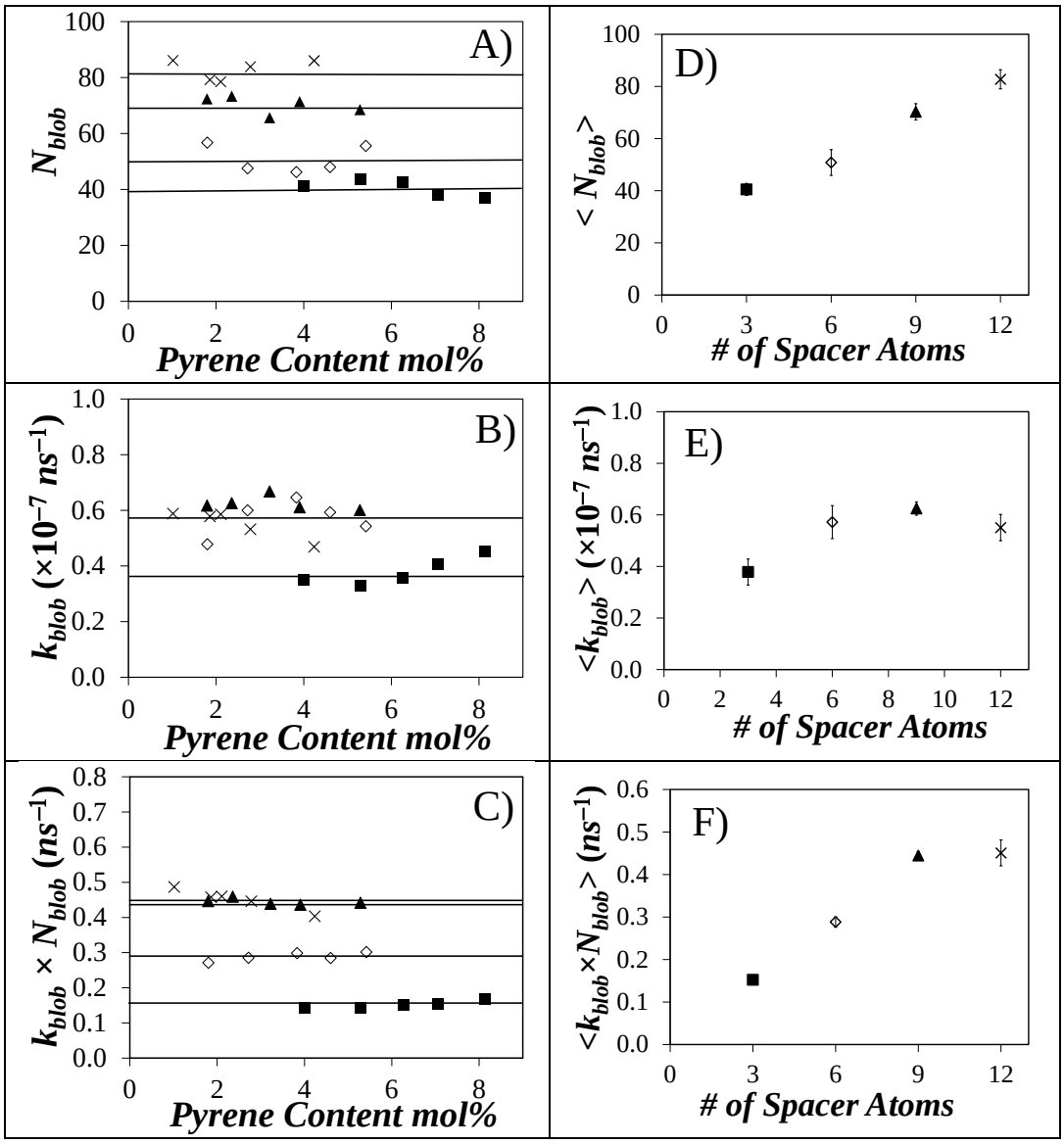

Figure 3. Plot of A) N_{blob}, B) k_{blob}, and C) $k_{blob} \times N_{blob}$ as a function of pyrene content and D) $<N_{blob}>$, E) $<k_{blob}>$, and F) $<k_{blob} \times N_{blob}>$ as a function of the number of spacer atoms for (■) $PyEG_0PBMA$ labeled with 4.0, 5.3, 6.3, 7.1, and 8.1 mol% pyrene, (◇) $PyEG_1PBMA$ labeled

with 1.8, 2.7, 3.8, 4.6 and 5.4 mol% pyrene, (■) $PyEG_2PBMA$ with 1.8, 2.3, 3.2, 3.9, and 5.3 mol% pyrene, and (×) $PyEG_3PBMA$ labeled with 1.0, 1.8, 2.1, 2.7, and 4.3 mol% pyrene in THF. $[Py] = 2.5 \times 10^{-6}$ M, $\lambda_{ex} = 344$ nm.

The behavior of $<k_{blob}>$ plotted as a function of the linker length in Figure 3E was quite remarkable. By definition, k_{blob} is equal to the product $k_{diff} \times [Py]_{blob}$ where k_{diff} is the bimolecular rate constant for diffusive encounters between two monomers bearing a pyrene group and $[Py]_{blob}$ is the local concentration equivalent to one ground-state pyrene inside a *blob* ($[Py]_{blob}=1/V_{blob}$). Since V_{blob} scales as $N_{blob}^{3\nu}$ where ν is the Flory exponent[23,24] equal to 0.6 in a good-solvent for PBMA like THF,[20] k_{blob} is expected to decrease with increasing N_{blob} as has been observed in a number of examples.[25,26] Yet instead of decreasing as the spacer length increased from 3 to 12 atoms and N_{blob} increased linearly from 40.5 for $PyEG_0$-PBMA to 82.7 for $PyEG_3$-PBMA, k_{blob} increased from 0.38 (±0.05)×10^7 s^{-1} for $PyEG_0$-PBMA to 0.57 (±0.06)×10^7 s^{-1} for $PyEG_1$-PBMA and it remained relatively constant and equal to 0.57 (±0.05)×10^7 s^{-1} for the $PyEG_x$-PBMA series with spacer length x equal to 1 – 3. This unexpected trend was attributed to the enhanced mobility afforded by the flexible oligo(ethylene glycol) linker.

With 1-pyrenemethanol used to prepare $PyEG_0$-PBMA, the pyrenyl unit is tightly held via an ester bond close to the PBMA backbone, severely hindering its mobility and ability to form an excimer, and thus strongly reducing k_{diff} and resulting in a small k_{blob} value. Introducing one ethylene glycol unit in the linker of $PyEG_0$-PBMA to obtain $PyEG_1$-PBMA enhances the mobility of the pyrene label considerably. This enhanced mobility is reflected by a much larger k_{diff} that counteracts the decrease in $[Py]_{loc}$ associated with the longer spacer, thus resulting in the increase of k_{blob} from 0.38 (±0.05)×10^7 s^{-1} for $PyEG_0$-PBMA to 0.57 (±0.06)×10^7 s^{-1} for $PyEG_1$-PBMA.

Addition of a second and third ethylene glycol unit further releases the steric constraints imposed by the main chain, but this effect decreases with each addition of an ethylene glycol unit in the spacer. Assuming that $[Py]_{loc}$ scales as $N_{blob}^{-1.8}$ ($[Py] = 1/V_{blob} \sim N_{blob}^{-3\nu}$) the effect that adding one ethylene glycol unit has on k_{diff} can be estimated by applying Equation 3 where x represents the number of ethylene glycol units in the linker.

$$\frac{k_{diff,x+1}}{k_{diff,x}} = \frac{k_{blob,x+1}}{k_{blob,x}} \times \left(\frac{N_{blob,x+1}}{N_{blob,x}} \right)^{1.8} \quad (3)$$

Based on the FBM parameters retrieved from the decay analysis and whose average values are shown in Figures 4D and 4E, Equation 3 predicts that k_{diff} increases by 2.3 ± 0.3, 2.0 ± 0.2, and 1.2 ± 0.1 when the linker length is increased from $PyEG_0$-PBMA to $PyEG_1$-PBMA, from $PyEG_1$-PBMA to $PyEG_2$-PBMA, and from $PyEG_2$-PBMA to $PyEG_3$-PBMA, respectively. According to this trend, addition of two ethylene glycol units to obtain $PyEG_2$-PBMA appears to provide the pyrene label with sufficient mobility to no longer sense the hindrance from the main chain, as adding a third ethylene glycol unit to the linker of $PyEG_2$-PBMA to generate $PyEG_3$-PBMA hardly changes k_{diff}, with the ratio $k_{diff,3}/k_{diff,2}$ taking a value close to unity (1.2 ± 0.1). While reducing steric hindrance enhances pyrene excimer formation, it must also be pointed out that it also reduces the response of pyrene to the dynamics of the main chain. Consequently these results indicate that in the case of PBMA, using a linker with 6 or less spacer atoms such as for $PyEG_0$-PBMA and $PyEG_1$-PBMA, pyrene excimer formation probes the dynamics of the main chain but that using a linker with 9 or more spacer atoms such as for $PyEG_2$-PBMA and $PyEG_3$-PBMA, pyrene excimer formation is more representative of the dynamics of the side chains rather than the dynamics of

the main chain. This information might be of particular interest for applying pyrene excimer formation to the study of branched macromolecules such as polymeric bottlebrushes where the side chains can be much longer than the longest spacer employed in this study for $PyEG_3$-PBMA.

The main consequence of having k_{blob} taking a larger but constant value for linkers made of a number x of EG units comprised between 1 and 3 is that the product $<k_{blob} \times N_{blob}>$ increased almost linearly with increasing linker length up to $x = 2$ before plateauing in Figure 3F for $x = 3$ instead of decreasing as $k_{diff} \times N_{blob}^{1-3\nu}$ as could be expected based on scaling argument alone.[25,26] While the interpretation of the trend obtained with $<k_{blob} \times N_{blob}>$ in Figure 3E is complicated by the fact that k_{blob} depends both on the *blob* volume via N_{blob} and the flexibility of the oligo(ethylene glycol) linker via k_{diff}, the trend obtained with N_{blob} in Figure 3D is more straightforward to interpret since N_{blob} relies solely on the volume V_{blob} probed by an excited pyrene label.

As a matter of fact, knowledge of the Mark-Houwink-Sakurada (MHS) parameters K and a for PBMA in THF enables the use of N_{blob} to estimate the hydrodynamic radius of a *blob*, R_{blob}, as a function of the number x of ethylene glycol units linking pyrene to the PBMA chain. Since the N_{blob} value ranging from 40 to 83 monomers would be equivalent to low molecular weight PBMA samples for which the MHS parameters were unavailable in THF at room temperature, they were determined by measuring the intrinsic viscosity at 25 °C of five PBMA samples having a narrow molecular weight distribution and with M_n values ranging between 2.5 and 38 K. The intrinsic viscosity experiments were conducted in THF at 25 °C. A plot of $[\eta]$ as a function of M_n is shown in Figure S10 in SI. A plot of $Ln[\eta]$ versus $Ln(M_n)$ could be well fitted with a straight line and the fit yielded the K and a parameters of the MHS equation found to equal 2.8 (±0.6)×10^{-4} mL/g and 1.09 ± 0.03, respectively. The parameters K and a were then introduced into Equation 4 to determine R_{blob}, the equivalent hydrodynamic radius of a *blob*.

$$R_{blob} = \left(\frac{3KN_{blob}^{a+1}}{10\pi N_A} \right)^{1/3} \quad (4)$$

A plot of R_{blob} as a function of the linker length is shown in Figure 4. Within experimental error, R_{blob} increased linearly by an increment δr of 0.32 ± 0.06 nm per ethylene glycol unit added to the linker.

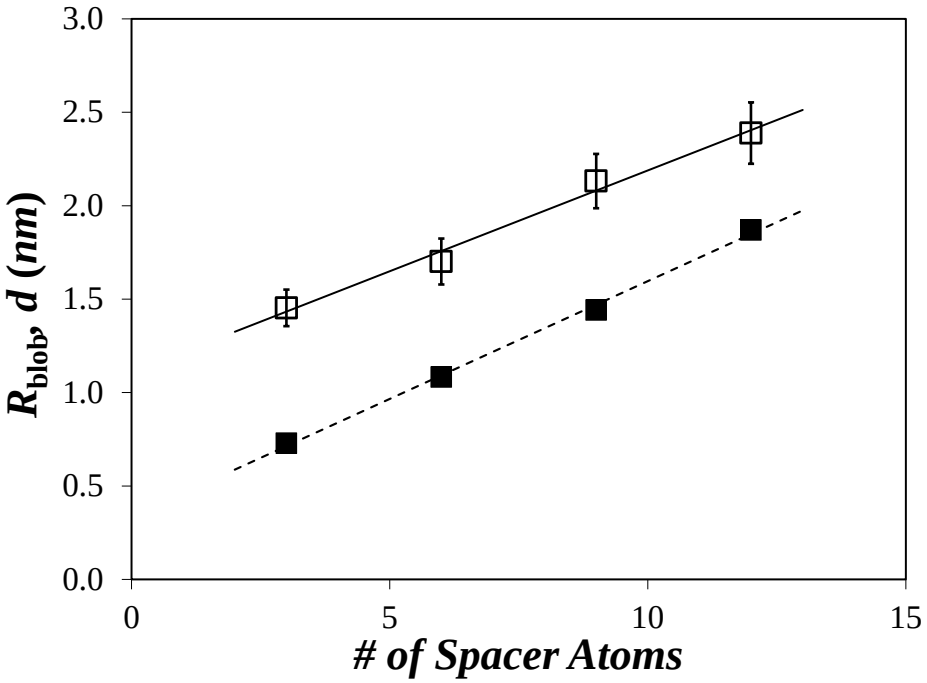

Figure 4. Comparison of R_{blob} (□) and the spacer length *d* (■) for the $PyEG_x$-PBMA series.

The increase in R_{blob} with increasing linker length could be accounted for, in part, by considering the end-to-end distance of the stretched oligo(ethylene glycol) spacer (*d*) between the carbon in the main PBMA chain bearing the carbonyl group to the center of the pyrene molecule. The distance *d* was calculated by conducting molecular mechanics optimizations with

HyperChem. The constructs generated through these optimizations can be viewed in Table S2. Plotting *d* as a function of the number of linker atoms yielded a straight line in Figure 4 with a slope of 0.126 nm/side chain atom, representing an increment δr of 0.38 nm per ethylene glycol unit similar to that found for R_{blob} (0.32 ± 0.06 nm per ethylene glycol unit). Since R_{blob} and *d* increased in a similar manner with increasing number of linker atoms, it strongly suggests that the increase in R_{blob} shown in Figure 3D was directly related to the increase δr = 0.38 nm in linker length brought about by each addition of an ethylene glycol unit.

DISCUSSION

The present study enables one to draw a direct comparison between the dynamics experienced by pyrene labels distributed randomly in a macromolecule according to two orthogonal structural arrangements. In the first arrangement, the pyrene labels are randomly distributed along a main chain but held at a same distance from the main chain via a butyl spacer while the length of the side chains increases from a methyl to a stearyl units (see Figure 5). To obtain this structural arrangement, 1-pyrenebutyl methacrylate was copolymerized with a series of alkyl methacrylates to yield the polymer samples Py-PCxMA where C*x* represents a linear alkyl side chain with *x* carbon atoms. The results of this study have been already published.[21] The second structural arrangment corresponds to the present study whereby a PBMA main chain is labeled randomly with pyrene held at increasing distances from the main chain via an oligo(ethylene glycol) spacer. These samples were referred to as $PyEG_x$-PBMA where $x = 0 – 3$ represents the number of ethylene glycol units in the side chain. As a matter of fact, the Py-PC*x*MA constructs enable one to monitor the dynamics experienced by a main chain as longer side chains are incorporated into the polymer

while the $PyEG_x$-PBMA series enables one to probe the dynamics experienced by the tip of a side chain growing perpendicularly to the main chain.

Py-PC*x*MA Series					
Py-PC1MA	**Py-PC4MA**	**Py-PC6MA**	**Py-PC8MA**	**Py-PC12MA**	**Py-PC18MA**
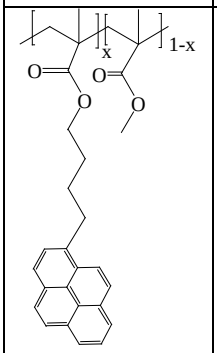	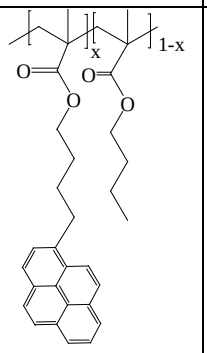	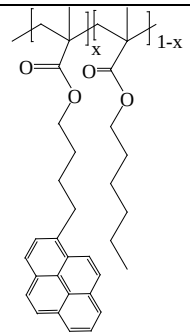	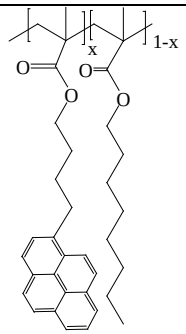	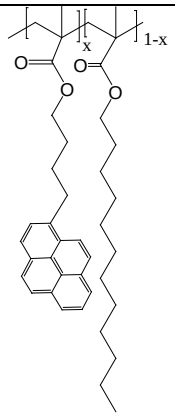	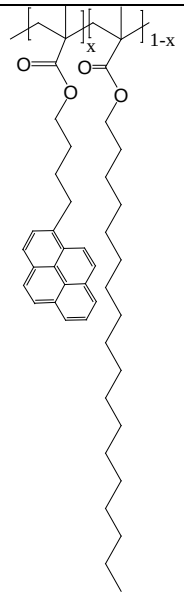

$PyEG_x$-PBMA Series			
$PyEG_0$-PBMA	**$PyEG_1$-PBMA**	**$PyEG_2$-PBMA**	**$PyEG_3$-PBMA**
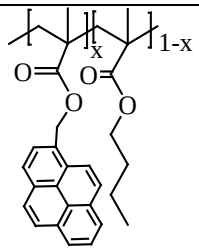	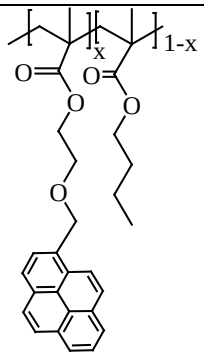	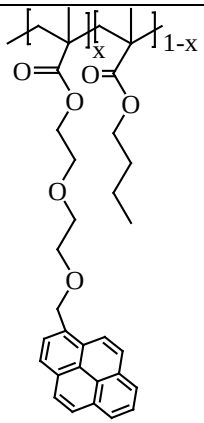	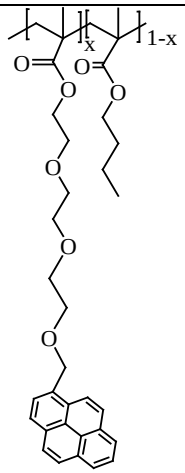

Figure 5. Comparison of the chemical structure of the Py-PC*x*MA and PyEG$_x$-PBMA samples that were studied in ref #21 and the present report, respectively.

As shown in Figure 6, all parameters retrieved from the analysis of the fluorescence data show strikingly different trends depending on the structural arrangement of the pyrene labels when plotted as a function of the number of side chain atoms. All parameters indicate that excimer formation is strongly reduced when the side chain length is increased for the Py-PC*x*MA series. As the side chain length increases, the efficiency of excimer formation reflected by $m(I_E/I_M)$ decreases in Figure 6A. This effect is due to the smaller *blob* volume V_{blob}, as reflected by the decreasing N_{blob} value in Figure 6B, probed by an excited pyrene as the motion of the label is hindered by the bulkier substituents and slower main chain mobility. Similarly, the dynamics of the main chain probed by the decreasing $<k_{blob}\times N_{blob}>$ product in Figure 6C are strongly slowed down by the larger substituents.

By comparison, an increase in the length of the oligo(ethylene glycol) side chain bearing the 1-pyrenemethoxy label in the PyEG$_x$-PBMA series is associated with a substantial enhancement in excimer formation as illustrated in Figure 6A for $m(I_E/I_M)$. The reason for this increased excimer formation is the larger reach of the tip of the side chain that allows an excited pyrene to probe a larger V_{blob} reflected by a larger N_{blob} in Figure 6B, as well as faster dynamics due to reduced steric hindrance from the main chain as illustrated in Figure 6C where the product $<k_{blob}\times N_{blob}>$ increased with increasing side chain length. Based on the trends described in Figure 6, the substantial difference in behaviour observed between the fluorescence data obtained for the Py-PC*x*MA and PyEG$_x$-PBMA series represents a strong indication that pyrene excimer

fluorescence measurements can provide valuable information about the dynamics experienced by a HBM along and perpendicularly to its main chain.

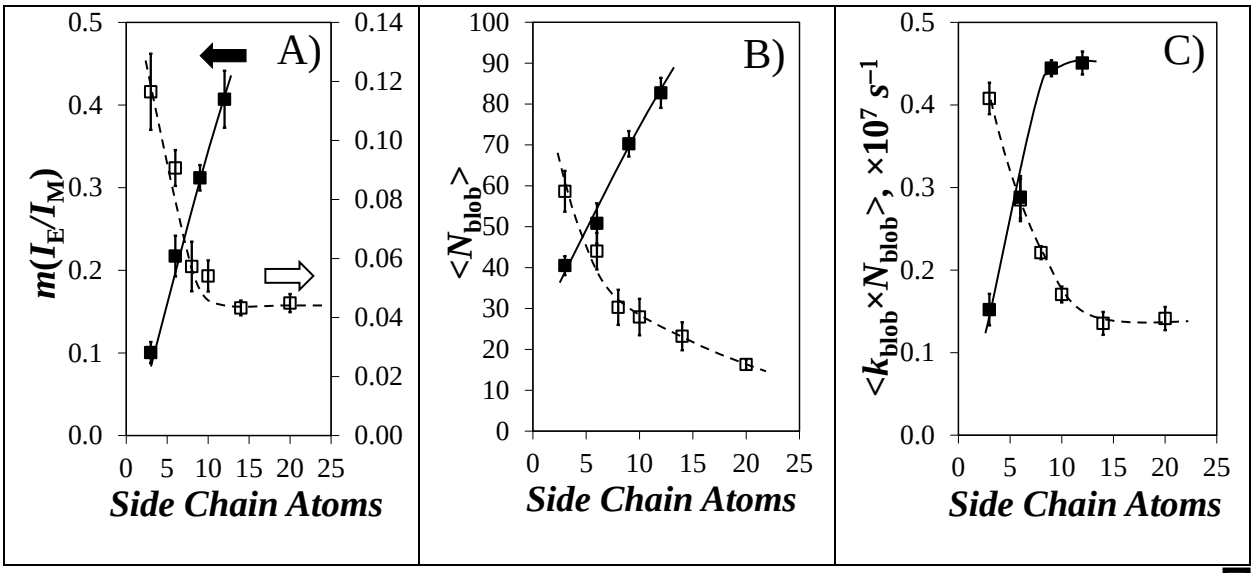

Figure 6. Plot of $m(I_E/I_M)$, $<N_{blob}>$, and $<k_{blob} \times N_{blob}>$ as a function of side chain atoms for the (□) Py-PC*x*MA and (■) $PyEG_x$-PBMA series.

CONCLUSIONS

This study has demonstrated that excimer formation between pyrene labels covalently attached to the tip of side chains responds quite strongly to the size of the linker connecting pyrene to the main chain in terms of both increased mobility characterized by k_{blob} and enhanced reach within the polymer coil as described by R_{blob}. Both effects contributed to dramatically increase pyrene excimer formation as found from the analysis of the steady-state fluorescence spectra through the I_E/I_M ratio (Figures 1 and 2). As a matter of fact, increasing the length of the linker connecting pyrene to the PBMA backbone resulted in the decoupling of the motion of the pyrene label in solution from that of the polymer main chain. The measurements described herein suggest that two ethylene glycol units between the pyrenemethoxy label and the polymethacrylate backbone are

required to achieve this decoupling. For linkers made of two or more ethylene glycol units, k_{blob} retrieved from the global FBM analysis of the fluorescence decays described mainly the diffusive motion of the side chains whereas N_{blob} provided a measure of the volume probed by the tip of the side chains. For shorter side chains, k_{blob} reflected the diffusive motion of the main chain. These observations are important to design a proper linker between a dye and a linear polymer depending on the element of a macromolecule (main chain versus side chain) being investigated.

The volume described by the tip of the side chains within the polymer coil could be determined quantitatively by applying the MHS equation to the N_{blob} values retrieved from the FBM analysis of the decays to yield R_{blob}, the hydrodynamic radius of a *blob*. While k_{blob} increased with increasing side chain length due to the relaxation of the dye as it was more separated from the main chain, the increase in R_{blob} by an increment of 0.38 nm per added ethylene glycol unit with increasing linker length could be mostly accounted for by considering the increase in length of the extended linker determined from molecular mechanics optimizations carried out with HyperChem.

The conclusions reached in the present study regarding the volume probed by the tip of a side chain and its dynamics were enabled by the FBM whose framework readily distinguishes between the contributions of the different pyrene species present in solution and the process of excimer formation due to the different length and time scales experienced by an excited pyrene attached to the tip of a series of side chains. The results presented herein suggest that pyrene excimer formation should be a powerful tool for the study of HBMs such as comb polymers or polymeric bottlebrushes. Using a short and long linker to connect pyrene to the macromolecule enables the experimentalist to probe the dynamics along and perpendicular to the main chain,

respectively, a feature that should prove extremely useful to the many scientists interested in characterizing HBMs at the molecular level.

ACKNOWLEDGEMENTS

SF and JD thank Mario Gauthier, Remi Casier, and Eric Morales for helpful suggestions regarding the synthesis of the $PyEG_x$-OH compounds with $x = 0 – 3$. SF and JD are also most grateful to NSERC for financial support.

SUPPORTING INFORMATION

Description of the Fluorescence Blob Model (FBM), ^{1}H NMR spectra of $PyEG_2$-OH, $PyEG_3$-OH, $PyEG_o$-MA, $PyEG_2$-MA, and $PyEG_3$-MA, fluorescence spectra of the $PyEG_x$-PBMA samples, intrinsic viscosity measurements, distances determined by molecular mechanics optimization, parameters retrieved from the FBM analysis of the fluorescence decays, references.

REFERENCES

1. Beers, K. L.; Gaynor, S. G.; Matyjaszewski, K.; Sheiko, S. S.; Möller, M. The Synthesis of Densely Grafted Copolymers by Atom Transfer Radical Polymerization. *Macromolecules* **1998**, *31*, 9413-9415.
2. Lee, H.-I.; Pietrasik, J.; Sheiko, S. S.; Matyjaszewski, K. Stimuli-Responsive Molecular Brushes. *Prog. Polym. Sci.* **2010**, *35*, 24-44.

3. Stals, P. J. M.; Li, Y.; Burdyska, J.; Nicolÿ, R.; Nese, A.; Palmans, A. R. A.; Meijer, E. W.; Matyjaszewski, K.; Sheiko, S. S. How Far Can We Push Polymer Architecture? *J. Am. Chem. Soc.* **2013**, *135*, 11421-11424.
4. He, Y.-M.; Feng, Y.; Fan, Q.-H. Asymmetric Hydrogenation in the Core of Dendrimers. *Acc. Chem. Res.* **2014**, *47*, 2894-2906.
5. Caminade, A.-M.; Turrin, C.-O. Dendrimers for Drug Delivery. *J. Mater. Chem. B* **2014**, *2*, 4055-4066.
6. Hadjichristidis, N.; Pitsikalis, M.; Iatrou, H.; Pispas, S. The Strength of the Macromonomer Strategy for Complex Macromolecular Architecture: Molecular Characterization, Properties, and Applications of Polymacromonomers. *Macromol. Rapid Comm.* **2003**, *24*, 979-1013.
7. Gauthier, M. Arborescent Polymers and Other Dendigraft Polymers: A Journey into Structural Diversity. *J. Polym. Sci. A*: *Polym. Chem.* **2007**, *45*, 3803-3810.
8. Seog, J.; Dean, D.; Plaas, A. H. K.; Wong-Palms, S.; Grodzinsky, A. J.; Ortiz, C. Direct Measurement of Glycosaminoglycan Intermolecular Interactions via High Resolution Force Spectroscopy. *Macromolecules* **2002**, *35*, 5601-5615.
9. McNelles, S. A.; Knight, S. D.; Janzen, N.; Valliant, J. F.; Adronov, A. Synthesis, Radiolabeling, and In Vivo Imaging of PEGylated High Generation Polyester Dendrimers. *Biomacromolecules* **2015**, *16*, 3033-3041.
10. Olesen, K. R.; Bassett, D. R.; Wilkerson, C. L. Surfactant Co-Thickening in Model Associative Polymers. *Prog. Org. Coatings* **1998**, *35*, 161-170.
11. Wang, X.; Guerrand, L.; Wu, B.; Li, X.; Boldon, L.; Chen, W.-R.; Liu, L. Characterizations of Polyamidoamine Dendrimers with Scattering Techniques. *Polymers* **2012**, *4*, 600-616.

12. Caminade, A.-M.; Laurent, R.; Majoral, J.-P. Characterization of Dendrimers. *Adv. Drug Delivery Rev.* **2005**, *57*, 2130-2146.
13. Sheiko, S. S.; Möller, M. Visualization of Macromolecules – A First Step to Manipulation and Controlled Response. *Chem. Rev.* **2001**, *101*, 4099-4123.
14. Mathew, A.; Siu, H.; Duhamel, J. A *Blob* Model to Study Chain Folding by Fluorescence. *Macromolecules* **1999**, *32*, 7100-7108.
15. Duhamel, J. Polymer Chain Dynamics in Solution Probed with a Fluorescence Blob Model *Acc. Chem. Res.* **2006**, *39*, 953-960.
16. Duhamel, J. New Insights in the Study of Pyrene Excimer Fluorescence to Characterize Macromolecules and their Supramolecular Assemblies in Solution. *Langmuir* **2012**, *28*, 6527-6538.
17. Duhamel, J. Global Analysis of Fluorescence Decays to Probe the Internal Dynamics of Fluorescently Labeled Macromolecules. *Langmuir* **2014**, *30*, 2307-2324.
18. Winnik, M. A.; Redpath, T.; Richards, D. H. The Dynamics of End-to-End Cyclization in Polystyrene Probed by Pyrene Excimer Formation. *Macromolecules* **1980**, *13*, 328-335.
19. Winnik, M. A. End-to-End Cyclization of Polymer Chains. *Acc. Chem. Res.* **1985**, *18*, 73-79.
20. Farhangi, S.; Duhamel, J. A Pyrenyl Derivative with a Four Atom-Linker that Can Probe the Local Polarity of Pyrene-Labeled Macromolecules. *Submitted to J. Phys. Chem. B* **2015**.
21. Farhangi, S.; Weiss, H.; Duhamel, J. Effect of Side-Chain Length on the Polymer Chain Dynamics of Poly (Alkyl Methacrylate) s in Solution. *Macromolecules* **2013**, *46*, 9738-9747.

22. Zaragoza-Galán, G.; Fowler, M.; Duhamel, J.; Rein, R.; Solladié, N.; Rivera, E. Synthesis and Characterization of Novel Pyrene-Dendronized Porphyrins Exhibiting Efficient Fluorescence Resonance Energy Transfer (FRET): Optical and Photophysical Properties. *Langmuir* **2012**, *28*, 11195-11205.
23. Flory, P. J.; Principles of Polymer Chemistry, Cornell University Press, 1953.
24. De Gennes, P.-G. Scaling Concepts in Polymer Physics, Cornell University Press, 1979.
25. Kanagalingam, S.; Spartalis, J.; Cao, T.-C.; Duhamel, J. Scaling Relations Related to the Kinetics of Excimer Formation between Pyrene Groups Attached onto Poly(N,N-dimethylacrylamide)s. *Macromolecules* **2002**, *35*, 8571-8577.
26. Irondi, K.; Zhang, M.; Duhamel, J. Study of the Semidilute Solutions of Poly(*N*,*N*-dimethylacrylamide) by Fluorescence and its Implications to the kinetics of Coil-to-Globule Transitions. *J. Phys. Chem. B*, **2006**, *110*, 2628-2637.

Table of Content